Journal of Hip Preservation Surgery, 2024, **11**, 20–29
DOI: https://doi.org/10.1093/jhps/hnad037
Advance access publication date: 11 November 2023
Research article

Development of a simulation system for femoroacetabular impingement detection based on 3D images

Chun-Ming Chen[1], Shang-Chih Lin[1,2], Chen-Te Wu[3] and Yi-Sheng Chan[4,5,6*]

[1]Taiwan High Speed 3D Printing Research Center, National Taiwan University of Science and Technology, No. 43, Sec. 4, Keelung Rd., Da'an Dist., Taipei, Taiwan , [2]Graduate Institute of Biomedical Engineering, National Taiwan University of Science and Technology, No. 43, Sec. 4, Keelung Rd., Da'an Dist., Taipei, Taiwan , [3]Department of Medical Imaging and Intervention, Chang Gung Memorial Hospital, No. 5, Fuxing St., Guishan Dist., Taoyuan, Taiwan , [4]Department of Orthopedic Surgery, Chang Gung Memorial Hospital, No. 222, Maijin Rd., Anle Dist., Keelung, Taiwan, [5]Comprehensive Sports Medicine Center, Chang Gung Memorial Hospital, No. 5, Fuxing St., Guishan Dist., Taoyaun, Taiwan and [6]Bone and Joint Research Center, Chang Gung Memorial Hospital, No. 5, Fuxing St., Guishan Dist., Taoyuan, Taiwan

*Correspondence to: Y.-S. Chan. E-mail: yschan512@gmail.com

ABSTRACT

Image-based criteria have been adopted to diagnose femoroacetabular impingement (FAI). However, the overlapping property of the two-dimensional X-ray outlines and static and supine posture of taking computed tomography (CT) and magnetic resonance imaging images potentially affect the accuracy of the criteria. This study developed a CT image–based dynamic criterion to effectively simulate FAI, thereby providing a basis for physicians to perform pre-operative planning for arthroscopic surgery. Post-operative CT images of 20 patients with satisfactory surgical results were collected, and 10 sets of models were used to define the flexion rotation centre (FRC) of the three-dimensional FAI model. First, let these 10 groups of models simulate the FAI detection action and find the best centre offset, and then FRC is the result of averaging these 10 groups of best displacements. The model was validated in 10 additional patients. Finally, through the adjustment basis of FRC, the remaining 10 sets of models can find out the potential position of FAI during the dynamic simulation process. Rotational collisions detected using FRC indicate that the patient's post-operative flexion angle may reach 120° or greater, which is close to the actual result. The recommended surgical range of the diagnostic system (average length of 6.4 mm, width of 4.1 mm and depth of 3.2 mm) is smaller than the actual surgical results, which prevents the doctor from performing excessive resection operations, which may preserve more bones. The FRC diagnostic system detects the distribution of FAI in a simple manner. It can be used as a pre-operative diagnosis reference for clinicians, hoping to improve the effect and accuracy of debridement surgery.

INTRODUCTION

In terms of contact characteristics, femoroacetabular impingement (FAI) can be divided into three basic types: pincer, cam and mixed [1]. Most cases of FAI are caused by hypertrophic bone in the acetabulum or femoral head–neck junction. Not only does this extra bone affect the angle of motion, but it can also cause discomfort and damage to other tissues [2–4]. Typically, during clinical examination, the femur will rotate in multiple directions during the impingement test. Considering that bone hyperplasia often occurs in the anterior upper part of the femur, there are two most commonly used actions to detect impingement: (i) pure femur flexion to see if it reaches more than 120° and (ii) placing the hip joint at 90° flexion and internal rotation [5–7]. Other image-based tests have been developed to visually assess the extent of FAI using X-ray [8, 9], magnetic resonance imaging [10, 11] and computed tomography (CT) [12, 13] images.

During arthroscopic resection, the surgeon may use pre-operative images, such as the two-dimensional (2D) X-ray image in Fig. 1A or the three-dimensional (3D) model (Fig. 1B) plan surgical procedure [14]. However, the accuracy of clinical outcomes based on criteria interpreted using imaging information remains controversial [15, 16]. When identifying the outer contour of the pelvis from the patient's anterior–posterior direction, the most prominent contour lines can be seen. However, most of the protruding parts are anterior or posterior to the patient, which is not easy to judge at first glance. When presented only through 2D images, there will be a problem of overlapping contour feature lines [7, 17, 18]. Moreover, these image-based tests are only static evaluations in upright standing or supine postures, and the potential FAI location along the full hip articulation is unknown from these images. Consequently, the development of more accurate image-based criteria for diagnosing FAI is a topic that continues to be studied [19–27].

Typically, patients with FAI can have hypertrophic bone removed with minimally invasive arthroscopic surgery. Doctors must determine whether an adequate amount of bone has been removed through various means, such as using multiple 2D X-rays in different planes or employing dynamic assessments.

Submitted 26 July 2022; Revised 17 September 2023; revised version accepted 8 November 2023

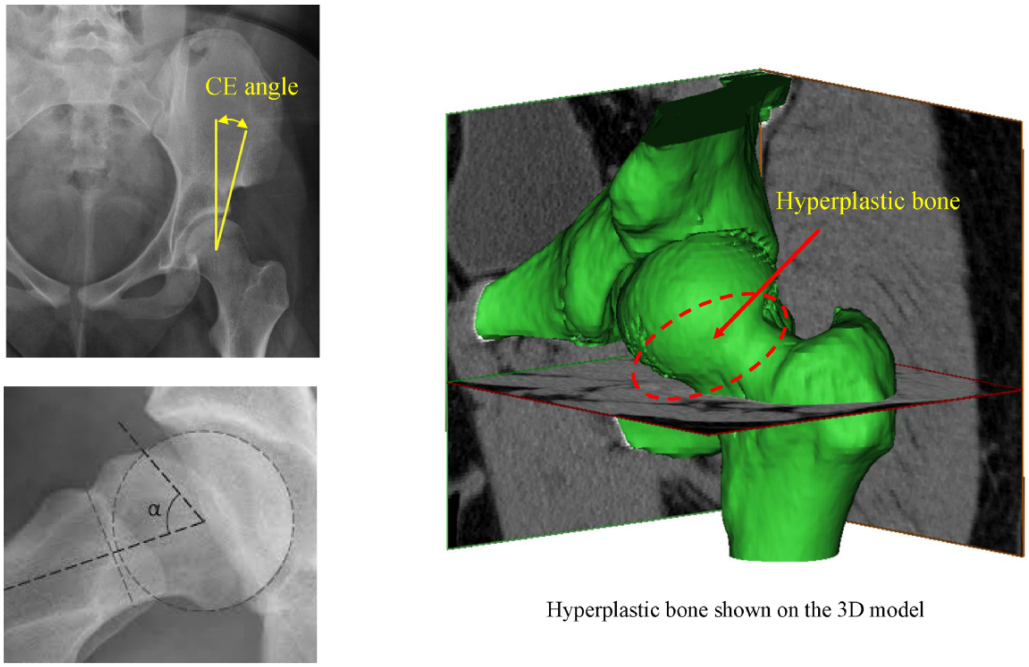

Fig. 1. The image information of FAI disease. (A) Two angle measurements on the 2D image. (B) The patient's hyperplastic bone is shown as a 3D model.

During the procedure, the femur was also rotated for an impingement test to confirm the adequacy of post-operative rotation or by using more advanced equipment, such as the Stryker HipCheck system. Sometimes in order to improve the post-operative experience of the patient, a little more bone is removed to prevent the patient from being unable to move the hip joint smoothly after the surgery. Therefore, if doctors can know the distribution of excess bone before surgery, the accuracy of arthroscopic surgery can be improved.

This study hypothesizes an ideal image-based standard to predict the overall location of FAI with two factors, that is, to find out the extent of hyperplastic bone distribution of FAI as much as possible and to provide doctors with a reference for detailed pre-operative planning. The first is to use the correct image to identify bone hyperplasia. The second is to understand the movement of the impingement test process in order to design a correct experimental programme.

MATERIAL AND METHODS

FAI patients

This is a retrospective study, approved by the Institutional Review Board (IRB 103-6645B), that randomly selected 20 patients (14 men and 6 women) who underwent FAI surgery and had good post-operative experience, as shown in Table I. The patients with 5 cam- and 15 mixed-type FAI diseases had undergone arthroscopic surgery. The visual analogue scale (VAS) for pain and modified Harris Hip Score (mHHS) for functional outcomes were assessed pre- and post-operatively. For all participating patients, the surgical outcomes of both VASs and mHHSs were satisfactory. Each patient took X-ray and CT images pre- and post-operatively. The α angle and centre-edge angle of the proximal femur were calculated from the X-ray images (Fig. 1A).

All scanning settings of the pre- and post-operative CT images were consistent with the 0.625-mm slice thickness and 120-kV and 260-mA environments to establish the standardized 3D reconstruction procedure. Using the commercial software Mimics (Materialise N.V., Leuven, Belgium) [25], CT images from the acetabulum to the trochanter were reconstructed into 3D models of the femur and pelvis, respectively.

Models

The model was divided into two independent mesh models, the femur and pelvis, which were further transformed into a solid model with smooth surfaces using SolidWorks software, version 2014 (SolidWorks Corporation, Concord, MA, USA) [26, 28]. Fig. 2A and B shows the pre- and post-operative arthroscopic and 2D images of FAI patients, as well as the use of post-operative models to simulate hip joint movement. The CT data of 20 patients collected during this research were reconstructed into pre- and post-operative 3D models, which were then randomly divided into two groups. The first group of patients was numbered 1–10, and the second group of models was numbered 11–20. 3D hip models reconstructed from 2D CT images must include the extra bone hyperplasia of the femoral and acetabular bones.

The femur and pelvis were divided into multiple regions to analyse the distribution of FAI. Using different systems for the two bones, there is less confusion when presenting the results.

Table I. ***The surgery information and the diagnostic criteria of the alpha angle and CE angle of 20 patients***

Patients	*Age (years)*	*Gender*	*Side*	*FAI type*	*α angle*	*CE angle*
1	59	Male	Left	Mixed	112.5	46.7
2	54	Male	Left	Mixed	77.6	33.7
3	59	Male	Left	Mixed	54.8	34.9
4	58	Male	Right	Mixed	61.7	41.8
5	39	Male	Right	Mixed	54.4	37.2
6	65	Male	Right	Mixed	92.7	37.9
7	23	Male	Right	Cam	53.2	34.1
8	38	Male	Left	Mixed	64.8	37.9
9	36	Female	Right	Cam	43.8	33.0
10	49	Male	Right	Mixed	74.1	35.5
11	26	Female	Right	Cam	64.7	35.2
12	56	Female	Left	Mixed	72.6	34.2
13	25	Female	Right	Mixed	63.2	53.3
14	40	Male	Left	Mixed	60.2	37.1
15	51	Male	Right	Mixed	82.7	37.9
16	56	Male	Left	Mixed	70.6	32.7
17	30	Female	Right	Cam	68.7	34.2
18	43	Male	Right	Mixed	70.1	33.6
19	33	Female	Right	Cam	45.8	33.4
20	54	Male	Left	Mixed	74.6	31.7

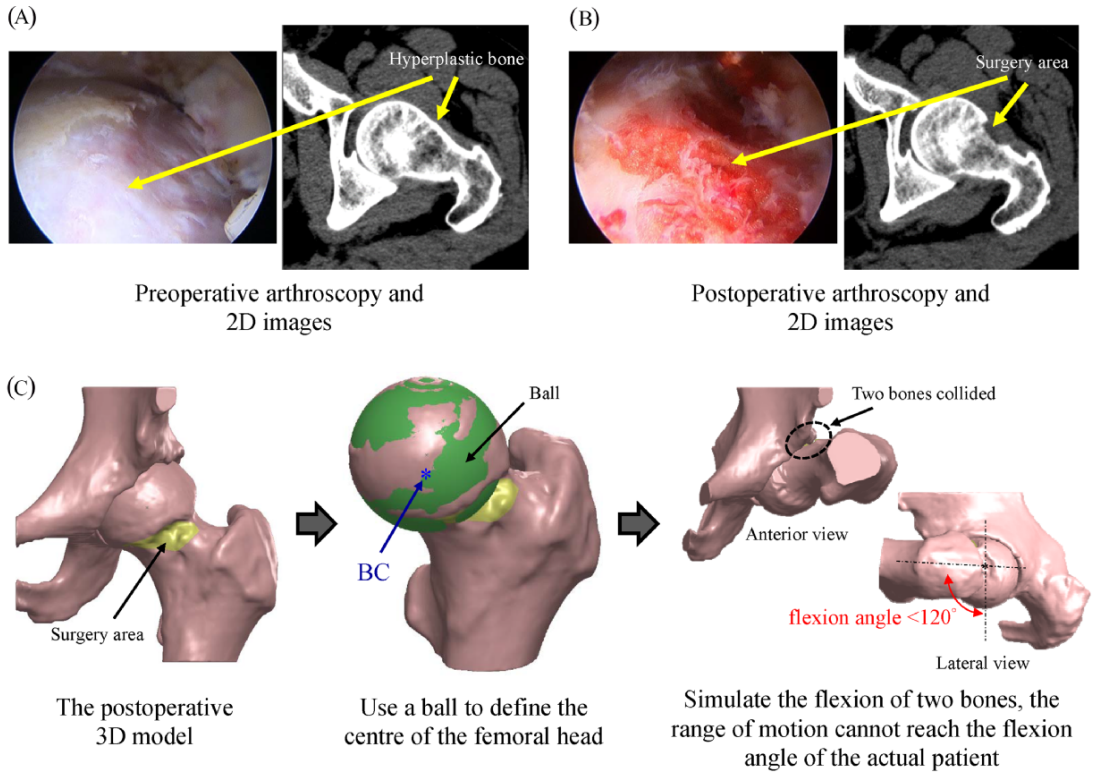

Fig. 2. Pre- and post-operative images and simulated movement. (A) Pre-operative arthroscopy and 2D images of the FAI patient. (B) Post-operative arthroscopy and 2D images of the FAI patient. (C) Post-operative model used to simulate hip joint movement.

The area around the femur head was divided into 12 regions clockwise 1–12 h: 12 h is cephalad, that is, on the superior of the femoral head, and 3 h was on the anterior side. The operative fields for these 20 patients were approximately distributed between 1 and 4 h. The pelvis was also divided into 12 regions around a 360° circle with labels set every 30°; the initial 0° was on the superior side, and 90° was on the anterior side of the pelvis.

FAI dynamic simulation

The FAI impingement test method was applied when the patients were lying down. The simulated movement method is divided

into two types according to the impingement test: (i) pure flexion and (ii) internal rotation after 90° flexion. In the simulation of the first pure flexion movement, the rotation angle was not predetermined. The femoral model continued to rotate during the flexion process until it automatically stopped when the two bones made contact. The second movement involved flexing to 90° followed by internal rotation. Similarly, the rotation angle was not pre-set but automatically ceased upon contact between the two bones, and rotation angles were recorded only when both came to a stop. Common areas of bony hypertrophy are typically located in the anterior and superior portions of the femur [5–7]. Therefore, in this study, the anterior side, where FAI occurs most frequently, was used as the target area for the simulated motion, during which 120° of flexion could be achieved.

Since the femoral head is rarely spherical, a fitting method is usually used to find the centre of the femoral head. We use the most common method, using a ball with a diameter similar to the size of the femoral head, then superimposing and aligning the two, taking the position with the smallest contour error and finally using the centre coordinates of the ball as the centre of the femoral head. When the ball centre (BC) is used as the centre of rotation, the obtained flexion angle will be smaller than the actual flexion angle of the post-operative patient. The simulation process is shown in Fig. 2C. It may be that the femur not only moves around the centre but also slides between the femur and the pelvis [29–33]. Therefore, it is desirable to find a centre of rotation that can represent the FAI test effect by an equivalent method. A 3D-printed post-operative 'specimen' was first applied to simulate motion, and a slight lateral and anterior positional slip of the femoral head was observed during flexion. Therefore, we applied the concept of sliding to simulations in the computer and performed calculations using post-operative phantoms of patients 1–10. Since the primary motion in impingement testing is flexion, this new centre of rotation is called the flexion rotation centre (FRC). Fig. 3 shows the flow of this study, from reconstructing the 3D model to defining a new centre of rotation FRC and verifying its correctness. Each post-operative model first finds its own BC and then targets flexion at 120°. By moving the coordinates of BC outward and forward by a certain distance, a new BC (NBC) can be found as the rotation centre of the model, thus reaching the goal (Fig. 4A–C). Finally, based on the average of 10 sets of NBC offset distances, the FRC for constructing the dynamic imaging system was defined.

This study used the FRC system to diagnose FAI symptoms from a pre-operative model of 11–20 patients. The hyperplastic bones of the femur and acetabulum interfere with each other after flexion to 120°. Thus, this study recorded the interference area of the two bones during movement. The distributions, lengths, widths and depths of the hyperplastic bones are labelled with different patterns. Fig. 4D and E show the diagnostic process and results of FAI when using the FRC system. Comparisons of 10 diagnostic results using FRC with self-models were reconstructed from the post-operative models of the patients numbered 11–20. To verify the accuracy of the FRC system, we checked whether the diagnostic area was consistent with the actual surgical outcome of the patients numbered 11–20.

This study's steps and focal points are briefly described as follows:

(i) Due to the hip joint not being an ideal ball-and-socket joint, it does not rotate around a fixed point.
(ii) Modelling the hip using this constraint causes premature impingement and reduced range of motion. This may be corrected by allowing the femoral head to displace from a fixed point as the femur rotates.
(iii) This study has developed a procedure that allows this displacement to occur within their computer model in concert with collision detection (via node separation). This increases allowable joint motion and yields more realistic values.
(iv) In this paper, we have taken solid models of 20 patients with limited hip motion who had their hip range of motion restored through bony resection of a cam lesion.
(v) The 20 patients were divided into two groups of 10 each. Using the first set of 10-person models, we determined the displacement required to allow hip joint flexion up to 120°. These 10 sets of head displacement changes were then combined and averaged to obtain a normalized head offset value.
(vi) We then imposed this standard displacement on each of the hip models in the second set of 10 computer models and measured simulated hip motion to bony impingement during two kinematic manoeuvres.

Deviation analysis

The results of the dynamic diagnosis system were compared with those of the post-operative 3D model, and the difference between the surgical site proposed by the FRC system and the actual result was calculated using PhysiGuide software, version 2.3.1 (Pou Yuen Technology Co., LTD, Changhua, Taiwan). Fig. 4E and F shows the overlap process, which integrates the 3D model after FRC collision detection with the actual post-operative 3D model. It calculates the closest distance between two nodes based on the pre-operative diagnostic model and the actual post-operative model.

Statistical methods

The chi-square test and Fisher's exact test were used for categorical variables. Student's t test was used for continuous variables. A two-tailed value of $P < 0.05$ was considered statistically significant. Each radiograph was evaluated by three skilled observers (two senior hip surgeons and one experienced radiologist) in a blinded fashion to assess interobserver and intraobserver variance. The observers classified the diagnosis of FAI type and measurement of the α angle and center-edge angle (CE angle) in 20 patients, and statistical analysis by the k method was used to determine the interobserver variance in the diagnosis of FAI type, α angle and CE angle. Intraobserver reliability was evaluated with a single-measure one-way random intraclass correlation coefficient with corresponding 95% confidence intervals. An a priori power analysis was conducted to ensure that certain conditions were met to correctly reject the null hypothesis, which stated that there is no relationship between the variables of interest. Statistical analysis was conducted by an independent

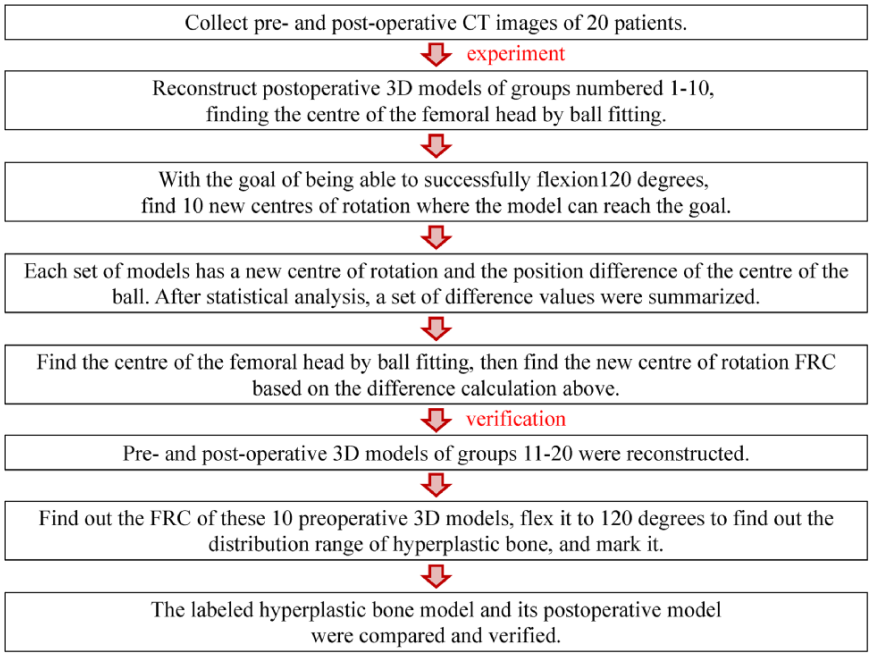

Fig. 3. 3D model reconstruction, definition and validation process for the new centre of rotation FRC.

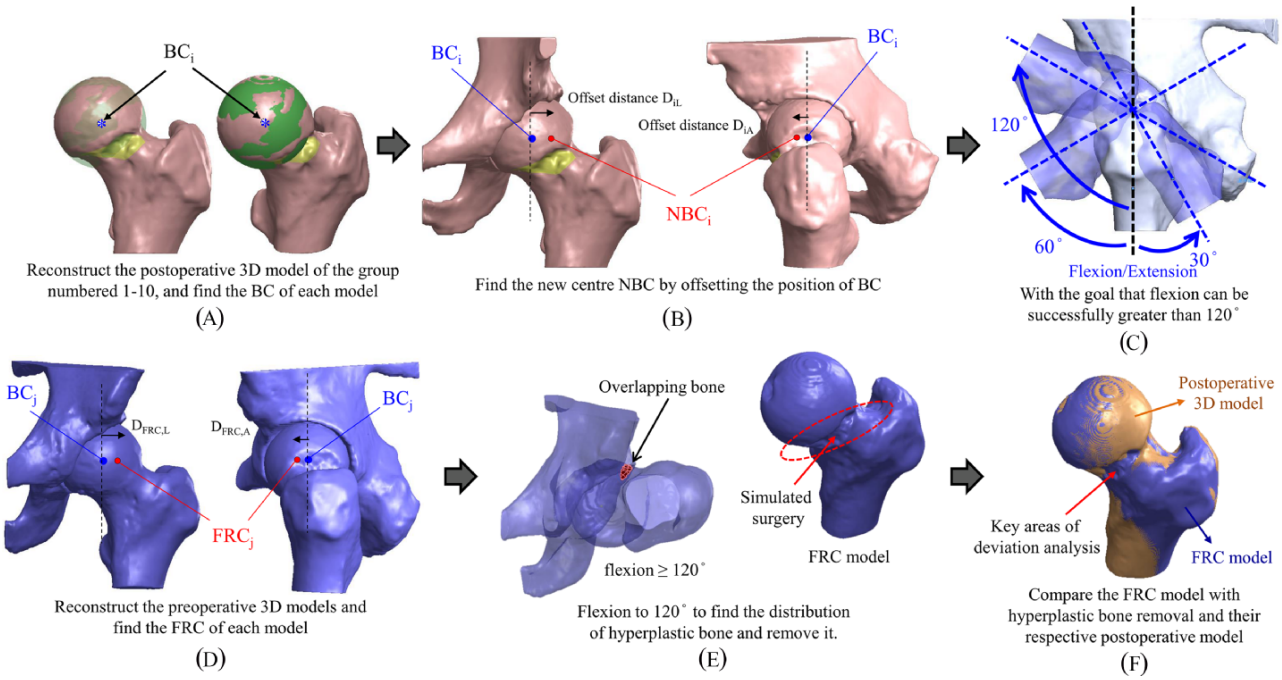

Fig. 4. The process of identifying and verifying FRCs. (A)–(C) Steps to find the NBC of each group of models. (D)–(F) Use FRC to find and remove hyperplastic bone and then compare the FRC model with the hyperplastic bone removed with the post-operative model of the patient.

statistical expert blinded to the surgical outcomes. The significance level was set at $P < 0.05$.

RESULTS

There were 20 patients with an average age of 38.5 years and an average follow-up time of 36 months. The VAS scores and mHHSs both showed significant improvement after surgery at the final follow-up (VAS from 5.6 to 1.1, mHHS from 61.0 to 93.4, all $P < 0.001$). Hip arthroscopy diagnoses and arthroscopic procedures in the 20 patients are listed in Table II. All patients with sports injuries returned to sports 6 months after the operation. The examinations during the post-operative follow-up all showed good conditions, with flexion angles reaching more than 120°. The results of additional diagnostic criteria, α angle and CE angle for FAI are listed in Table III. The regions of the repair surgery on the acetabular rim were in the range of 30–90°.

Table II. ***Hip arthroscopy diagnoses and arthroscopic procedures in the 20 patients***

	Data
Diagnosis, n (% of 20 hip arthroscopies)	
Mixed FAI	14 (70)
Isolated cam FAI	5 (25)
Isolated pincer FAI	1 (5)
Labral pathology	20 (100)
Cartilage pathology	11 (55)
Adhesions	1 (5)
Ligamentum teres pathology	5 (25)
Loose bodies	2 (10)
Arthroscopic procedure, n (% of 20 hip arthroscopic procedures)	
FAI procedure	20 (100)
Femoral osteoplasty	19 (95)
Acetabular rim trim	12 (60)
Labral procedure	20 (100)
Labral debridement	7 (35)
Labral repair	13 (65)
Cartilage procedure	11 (55)
Chondroplasty	5 (25)
Microfracture	9 (45)
Partial femoral head chondroplasty	2 (10)
Lysis of adhesions	1 (5)
Ligamentum teres procedure	5 (25)
Ligamentum teres debridement	5 (25)
Capsular procedure	4 (20)
Capsular plication	2 (10)
Thermal capsulorrhaphy	2 (10)
Loose body removal	2 (10)
Psoas release or lengthening	2 (10)

Table I shows that the average α angle of 20 patients was 72° (43.8–112.5°) and the average CE angle was 39° (33–53.3°). After follow-up for more than 2 years, the range of motion of all patients' hips achieved excellent functional results. The inter-observer variability in the diagnosis of FAI type, α angle and CE angle was insignificant in all cases ($P > 0.05$). The intraclass correlation coefficient values for the repeated measurements were above 0.9 at the lower bound of the 95% confidence interval for FAI type (0.91), α angle (0.94) and CE angle (0.92). Power analysis of this study was expressed as power = $1 - \beta$, where β is the probability of a type II error. The study had β equal to 0.1 and power equal to 0.92 (power should equal at least 0.80). Thus, the high power of 0.92 indicated that our study was worthwhile.

Comparison of different flexion movement types was performed for the post-operative 3D models of the patients numbered 11–20. Two types of movement modes were set. The first was pure flexion, where the action stopped when the interference collision occurred between the femoral and pelvic bone; the allowable rotation angle of flexion of all models was measured. The second mode was the internal rotation at 90° of flexion that simulated the FAI impingement test. This study also measured the allowable internal rotation angle when two bones stopped after generation of interference collision.

With BC as the centre of rotation, the average post-operative flexion angle of the 10 patients was 100.7° and the average internal rotation angle of the FAI impingement test was 14.1°, both of which were small. Using the results of rotational collision detection with the FRC system, the average post-operative flexion angle of the 10 patients was 128.3° and the average internal rotation angle of the FAI impingement test was 33.8°. The post-operative flexion degree of the patient can reach more than 120°, which is closer to the actual surgical effect of the patient. When the rotating reference was changed to the FRC system, the allowable rotation angle became larger. Compared to the BC centre of rotation, the flexion of the FRC system showed an average increase of 27.4% and the internal rotation was more than twice as high. The results of the allowable rotation angle are shown in Fig. 5.

The pre-operative 3D models of the patients numbered 11–20 were flexed to 120° using the FRC system, and the collision interference area between the two bones was found and removed. Thereafter, we integrated these models with the actual surgical models to calculate the maximum error of the bone shape. The results of the maximum error analysis are shown in Fig. 6. The minimal error of the two bones of these 10 patients was 3.1 mm, the maximum error was 9.7 mm and the average error was 5.6 mm. The range of hyperplastic bone resection recommended by the FRC diagnostic system is smaller than the actual surgical result, with an average length of less than 6.4 mm, a width of less than 4.1 mm and a depth of less than 3.2 mm. However, these models use the results of the FRC diagnostic system to simulate post-operative models. Their allowable rotation angle can be almost greater than 120°, so for the size of the removed bone, current surgery may remove too many bones.

DISCUSSION

FAI dynamic simulation

The main purpose of this research is to find a method that can effectively simulate the impingement test. Due to the recognition problem of overlapping features in 2D images [7, 17, 18]. Therefore, using 3D models to simulate flexion enables clinicians to understand areas of hyperplasia bone prior to surgery, hopefully reducing underestimation of hyperplastic bone. The generally common diagnostic methods of FAI discussed an α angle based on 2D images [19, 23, 34]. Although 3D methods have also been used for evaluating the hyperplasia of bones, in large part, the BC of the femoral head has been used for the rotation sets of the femur and pelvis. However, using the BC to represent the actual rotational motion of the human hip joint is an underestimate (Fig. 2C) [24–33].

The real hip joint movement is actually very complicated, but most of the research studies simplify it to the BC as the femoral centre of motion. This study found that in post-operative patients with the centre of the sphere as the centre of rotation of their model, the femur and pelvic femoral head collide when rotated approximately 90–100°. But for these patients who have undergone surgery, when they return to the outpatient clinic for follow-up, the flexion angle can reach more than 120° and the post-operative feedback is also very good. So, we think that the general centre of the ball cannot be used as the centre of rotation. Because of this, we used 3D printing to print out the bones to observe their kinematic relationship. When actually simulating the rotation of the two bones, it was found that if the rotation exceeds 120°, the femur must slide lateral and anterior. Since the

Table III. ***The distributed conditions of the hyperplastic bones of 20 patients and the marked regions for the femur and pelvis***

Patients	*Femur (12–4 h)*	*Pelvis (0–90°)*
1	1–4 h	30–60°
2	1–4 h	30–60°
3	2–3 h	45–75°
4	1–3 h	60–90°
5	2–3 h	60–75°
6	3–4 h	30–60°
7	3–4 h	60–75°
8	2–3 h	60–90°
9	2–4 h	60–90°
10	2–3 h	60–75°
11	3–4 h	60–90°
12	2–3 h	30–60°
13	2–3 h	30–60°
14	2–3 h	30–50°
15	3–4 h	60–75°
16	2–3 h	60–90°
17	1–3 h	60–90°
18	2–3 h	60–75°
19	3–4 h	60–90°
20	2–3 h	30–60°

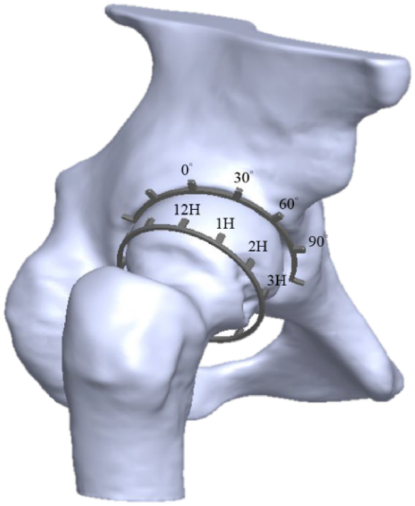

marked region

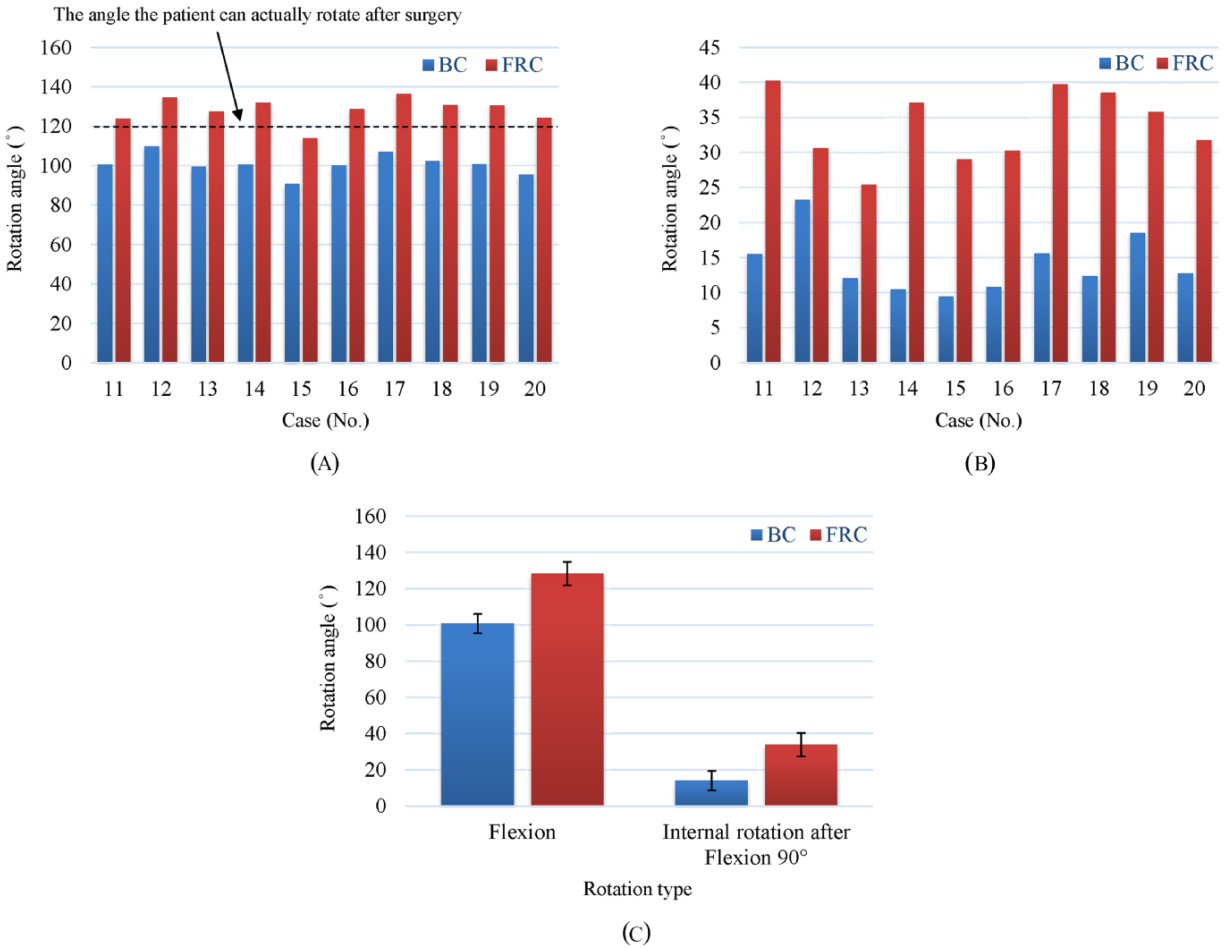

Fig. 5. Results of the first type verification: For the post-operative model numbered 11–20, two centres, BC and FRC, are used to simulate the results of these two movements. The angle of (A) flexion and (B) internal rotation after flexion 90°. (C) The average rotation angle of these two movements.

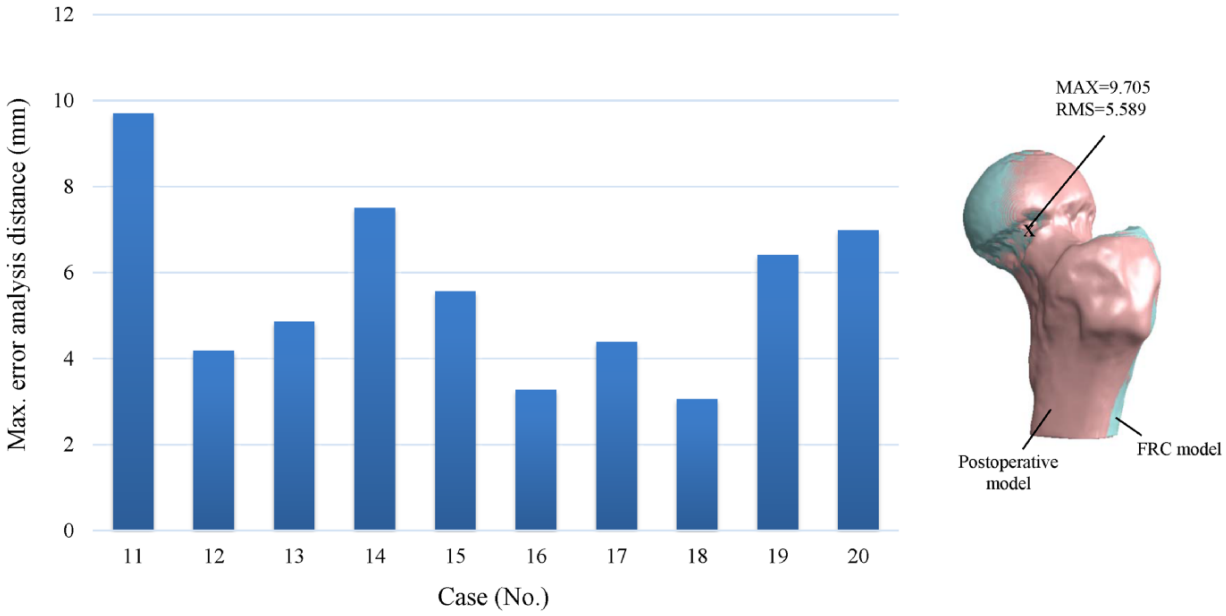

Fig. 6. The result of the second-type verification: for the pre-operative models of the 11–20 groups, the FRC was used for 120° flexion rotation to find and remove the hyperplastic bone, and then the FRC model with the hyperplastic bone removed and the patient's post-operative model were used for error analysis.

human femur and pelvis are not glued together but are wrapped in a layer of ligaments, the femur has room to slide as the hip rotates. Of course, many factors such as labrum, soft tissue, cartilage and sphericity will also cause differences in movement. But we just want to find out a general rule, we can try to compare the flexion situation, only the motion between two bones is considered and other tissues are not fully considered in this study.

When BC is the centre of rotation, the post-operative model collision detection angle is smaller than the actual post-operative angle, much smaller than 120°. However, the follow-up of these patients was good, and the post-operative flexion angle can return to normal flexion of more than 120°, without pain. Therefore, the collision results based on the BC will underestimate many areas of hyperplasia, which is not conducive to serving as the reference centre of femoral rotation for FAI testing. Because FAI most commonly occurs anterolateral, this study restricts the direction of motion to flexion based on diagnostic focus. Using the BC as a reference, 10 post-operative models were used to simulate flexion to 120° (Fig. 4C). Through this process, the centre of rotation that best represents the FAI test was found, the flexion rotation centre (FRC).

In this experiment, the models numbered 1–10 were repeatedly tested. After the first set of models go through different offset coordinates, the first suitable offset displacement will be found. A second set of models is introduced for testing. If you find that the two bones are still stuck when rotating, then continue to correct and find the appropriate offset. In this way, through 10 sets of models, iteratively find out the rotation centre of equivalent flexion. At this time, the offset between the coordinate position of the equivalent rotation centre and the original coordinate position is the difference that can be added when flexion each group of models. We use models numbered 1–10 to find out the displacement of the centre of rotation and then test it with 10 models numbered 11–20. The angle of flexion at the new centre of rotation was compared to the angle with the BC as the centre of rotation and compared to the actual post-operative results in patients 11–20. Since the patient can have greater than 120° of flexion in the subsequent impingement test, the results of the new centre of rotation are closer to real patients.

The allowable rotation angles of the FRC system were larger than the BC of the femoral head, and all of its angles could reach 120° or more (Fig. 5). Furthermore, these angles more closely approximate the patient's post-operative outcome. The main reason was that the FRC system estimated the rotating reference based on the actual post-operative models. While the FRC dynamic diagnostic system still only has a fixed centre of rotation for flexion, this will adjust the BC to certain lateral and anterior offsets. The FRC system takes sliding-related aspects into account during the flexion simulation step. The offset of the FRC only involves the movement to correct the coordinates of the centre of the femoral head. Since the corrected centre position is more suitable as the rotation reference centre for flexion motion, the rotation angle is more realistic.

Using this FRC diagnostic centre for pre-operative collision diagnosis, the region of interference between the two bones can be displayed in the 3D model (Fig. 5E). After quantifying the extent of this hyperplastic area, clinicians can clearly understand the extent of hyperplastic bone that needs to be resected pre-operatively, allowing for a clearer surgical plan earlier. There are also some studies using CT-based 3D model collision detection software to find the impingement area of FAI [35–38]. From

the literature results, it can be found that the impingement zone of the retroverted acetabulum is also mostly distributed in the anterior zone. As long as the hyperplastic bone is normally distributed in the anterior aspect, this FRC system should be able to detect it. However, the impingement area caused by acetabular protrusion is different from general FAI, and FRC may not be suitable.

Deviation analysis

The diagnostic system's measurement of hyperplastic bone is smaller than the actual surgical result. Diagnostic systems that may be based on anatomy assume that hip flexion should achieve an ideal 120° rotation as a criterion. The actual bone resection area for all patients was determined by the clinician using hip arthroscopy. In current clinical practice, as long as the width of the femoral neck remains within a safe range, clinicians remove more bone during surgery to restore adequate motion to the patient. Therefore, excessive bone resection can be reduced by providing clinicians with complete resection recommendations.

Limitations

This study has some limitations. First, the FRC system is only suitable for patients with FAI that occurs in the anterolateral region. Second, the data can only be used for pre-operative planning. In general, the target of FAI is hyperplastic bone tissue. The current study only acquired and used CT images to reconstruct a 3D model, which could not clearly identify cartilage tissue. Therefore, the results of this study were simulated only for the skeletal part. If magnetic resonance imaging images could be added as reference material for the model in the future, they could be considered in more detail together with the cartilage tissue.

CONCLUSIONS

In the FAI patients who underwent hip arthroscopy in this study, the distribution of hyperplastic bone was the same as shown in the literature, mainly in the anterolateral femur [7]. Referring to the motion mode setting of the impingement test, the diagnosis method of the Flexion Rotation Centre obtained by averaging 10 sets of model offsets is mainly used to find the rotation centre that can effectively present the flexion results. The system can detect the distribution of hyperplastic bone in the anterosuperior femur and in the pelvis. For patients who need FAI surgery, the 3D model is reconstructed first and then FRC is used to find the bone collision area. Collision results can also be 3D printed to create 3D specimens for surgeons to reference. Before surgery, the actual skeletal condition of the patient can be more intuitively understood to plan more detailed surgical procedures. This study hopes to find the most prevalent FAI distribution area by a simple method. If more patients with different FAI types are willing to participate in the future, the diagnostic system can be more comprehensively optimized.

DATA AVAILABILITY

All data generated or analysed during this study are included in this published article. The data that support the findings of this study are available from the Institutional Review Board (IRB 103-6645B), but restrictions apply to the availability of these data, which were used under licence for the current study.

ACKNOWLEDGEMENTS

The Chang Gung Memorial Hospital, National Taiwan University of Science and Technology and the Taiwan Ministry of Science and Technology provided partial support for this research. The number is MOST 104-2314-B-182A-015.

CONFLICT OF INTEREST STATEMENT

None declared.

REFERENCES

1. Kalesha N, Gina DP, Kawan R *et al.* Prevalence of cam-type femoroacetabular impingement morphology in asymptomatic volunteers. *J Bone Joint Surg* 2010; **92**: 2436–44.
2. Klaue K, Durnin CW, Ganz R. The acetabular rim syndrome: a clinical presentation of dysplasia of the hip. *J Bone Joint Surg* 1991; **73-B**: 423–9.
3. Reynolds D, Lucas J, Klaue K. Retroversion of the acetabulum: A cause of hip pain. *J Bone Joint Surg* 1999; **81-B**: 281–8.
4. Ito K, Minka-II MA, Leunig M *et al.* Femoroacetabular impingement and the cam-effect: a MRI-based quantitative anatomical study of the femoral head-neck offset. *J Bone Joint Surg* 2001; **83-B**: 171–6.
5. Leunig M, Beck M, Kalhor M *et al.* Fibrocystic changes at anterosuperior femoral neck: prevalence in hips with femoroacetabular impingement. *Radiology* 2005; **236**: 237–46.
6. Pfirrmann CW, Mengiardi B, Dora C *et al.* Cam and pincer femoroacetabular impingement: characteristic MR arthrographic findings in 50 patients. *Radiology* 2006; **240**: 778–85.
7. Tannast M, Goricki D, Beck M *et al.* Hip damage occurs at the zone of femoroacetabular impingement. *Clin OrthopRelat Res* 2008; **466**: 273–80.
8. Laborie LB, Lehmann TG, Engesæter I *et al.* The alpha angle in cam-type femoroacetabular impingement: new reference intervals based on 2038 healthy young adults. *Bone Joint J* 2014; **96-B**: 449–54.
9. Aaron C, Frank WG. Hip arthroscopy: common problems and solutions. *Clin Sports Med* 2018; **37**: 245–63.
10. Matthias L, Philipp AW, Christoph SP *et al.* Comparative study of the femoroacetabular impingement (FAI) prevalence in male semiprofessional and amateur soccer players. *Arthrosc Sports Med* 2014; **134**: 1135–41.
11. Angela EL, Shari TJ, Harry GG *et al.* MRI for the preoperative evaluation of femoroacetabular impingement. *Insights Imaging* 2016; **7**: 187–98.
12. Julian KC, Carl S, Chee G *et al.* Cam and pincer femoroacetabular impingement: CT findings of features resembling femoroacetabular impingement in a young population without symptoms. *AJR Am J Roentgenol* 2013; **200**: 389–95.
13. Rafal G, Daniel O, Kate S *et al.* Protocol for CT in the position of discomfort: preoperative assessment of femoroacetabular impingement – how we do it and what the surgeon wants to know. *J Med Imaging Radiat Oncol* 2014; **58**: 649–56.
14. Tannast M, Monika KL, Frank L *et al.* Noninvasive three-dimensional assessment of femoroacetabular impingement. *J Orthop Res* 2007; **25**: 122–31.
15. Nouh MR, Schweitzer ME, Rybak L *et al.* Femoroacetabular impingement: can the alpha angle be estimated? *AJR Am J Roentgenol* 2008; **190**: 1260–2.
16. Brian DG, Benjamin DK, Itay P *et al.* Acetabular morphologic characteristics predict early conversion to arthroplasty after isolated hip arthroscopy for femoroacetabular impingement. *Am J Sports Med* 2019; **48**: 188–96.

17. Sarah CF, Alan LZ, Jan N *et al.* Postoperative MRI findings and associated pain changes after arthroscopic surgery for femoroacetabular impingement. *AJR Am J Roentgenol* 2020; **214**: 177–84.
18. Joshua DH, Associate E. Editorial commentary: what exactly is impingementdCan dynamic magnetic resonance imaging 'See' impingement in femoroacetabular impingement? *Arthroscopy* 2019; **35**: 2375–9.
19. Nötzli HP, Wyss TF, Stoecklin CH *et al.* The contour of the femoral head-neck junction as a predictor for the risk of anterior impingement. *J Bone Joint Surg* 2002; **84-B**: 556–60.
20. Chan YS, Lien LC, Hsu HL *et al.* Evaluating hip labral tears using magnetic resonance arthrography: a prospective study comparing hip arthroscopy and magnetic resonance arthrography diagnosis. *Arthroscopy* 2005; **21**: 1250.e1–e8.
21. Anderson LA, Peters CL, Park BB *et al.* Acetabular cartilage delamination in femoroacetabular impingement: risk factors and magnetic resonance imaging diagnosis. *J Bone Joint Surg* 2009; **91**: 305–13.
22. Lohan DG, Seeger LL, Motamedi K *et al.* Cam-type femoral-acetabular impingement: is the alpha angle the best MR arthrography has to offer? *Skeletal Radiol* 2009; **38**: 855–62.
23. Rakhra KS, Sheikh AM, Allen D *et al.* Comparison of MRI alpha angle measurement planes in femoroacetabular impingement. *Clin Orthop Relat Res* 2009; **467**: 660–5.
24. Perreira AC, Hunter JC, Laird T *et al.* Multilevel measurement of acetabular version using 3-D CT-generated models. *Clin Orthop Relat Res* 2011; **469**: 552–61.
25. Eichelberg M, Riesmeier J, Wilkens T *et al.* Ten years of medical imaging standardization and prototypical implementation: the DICOM standard and the OFFIS DICOM toolkit (DCMTK). In: *Proc* Bellingham, Washington, USA: SPIE, Medical Imaging. Vol. 5371, 2004, pp. 57–68.
26. Garland M, Heckbert PS. Surface simplification using quadric error metrics. In: *SIGGRAPH 97 Conference Proceedings,* Los Angeles, California, United States of America August 3–8, 1997. pp. 209–16.
27. Sowmya V, Matthew PM, Fangbai W *et al.* The prevalence of athletic pubalgia imaging findings on MRI in patients with femoroacetabular impingement. *Skeletal Radiol* 2020; **49**: 1249–58.
28. Schroeder W, Zarge J, Lorensen W. Decimation of triangle meshes. *Comput Graph (SIGGRAPH' 92 Proceedings)* 1992; **26**: 65–70.
29. Piazza SJ, Erdemir A, Okita N *et al.* Assessment of the functional method of hip joint center location subject to reduced range of hip motion. *J Biomech* 2004; **37**: 349–56.
30. Delp SL, Maloney W. Effects of hip center location on the moment-generating capacity of the muscles. *J Biomech* 1993; **26**: 485–99.
31. Renata NK, Elsie GC, Patrick C *et al.* Radiographic and non-invasive determination of the hip joint center location: effect on hip joint moments. *Clin Biomech* 1999; **14**: 227–35.
32. Stagni R, Leardini A, Cappozzo A *et al.* Effects of hip joint centre mislocation on gait analysis results. *J Biomech* 2000; **33**: 1479–87.
33. Begon M, Monnet T, Lacouture P. Effects of movement for estimating the hip joint centre. *J Biomech* 2007; **25**: 353–9.
34. Meyer DC, Beck M, Ellis T *et al.* Comparison of six radiographic projections to assess femoral head/neck asphericity. *Clin Orthop Relat Res* 2006; **445**: 181–5.
35. Siebenrock KA, Steppacher SD, Haefeli PC *et al.* Valgus hip with high antetorsion causes pain through posterior extraarticular FAI. *Clin Orthop Relat Res* 2013; **471**: 3774–80.
36. Lerch TD, Boschung A, Todorski IAS *et al.* Femoroacetabular impingement patients with decreased femoral version have different impingement locations and intra- and extraarticular anterior subspine FAI on 3D-CT-based impingement simulation: implications for hip arthroscopy. *Am J Sports Med* 2019; **47**: 3120–32.
37. Lerch TD, Siegfried M, Schmaranzer F *et al.* Location of intra- and extra-articular hip impingement is different in patients with pincer-type and mixed-type femoroacetabular impingement due to acetabular retroversion or protrusio acetabuli on 3D CT-based impingement simulation. *Am J Sports Med* 2020; **48**: 661–72.
38. Joel W, Jeffrey JN, Karla CBS *et al.* Femoral morphology in the dysplastic hip: three-dimensional characterizations with CT. *Clin Orthop Relat Res* 2017; **475**: 1045–54.